

Special
Collection

Advanced Carbon Materials for Sodium-Ion Capacitors

Baowei Wang,^[a] Xu Gao,^[a] Laiqiang Xu,^[a] Kangyu Zou,^[a] Peng Cai,^[a] Xinglan Deng,^[a] Li Yang,^[a] Hongshuai Hou,^[a] Guoqiang Zou,^{*[a]} and Xiaobo Ji^[a]



Nonaqueous sodium-ion capacitors (SICs), as a new type of energy storage cell, can potentially achieve high energy-power densities, long cycling lifespan, and low cost in one device. Given this, developing suitable carbonaceous electrode materials for carbon-based SICs is of great significance. Unlike lithium-ion batteries (LIBs) and lithium-ion capacitors (LICs) that have been successfully commercialized, SICs are still at an early stage. As a result, rational electrode material design for SICs is needed to meet the requirements of electrochemical energy-storage systems. Carbon materials with a wide range of sources and low

toxicity deliver significant potential applications in high-performance SICs, whether as positive or negative parts. Various carbonaceous electrode materials have been explored and investigated for developing SICs over the past years. This Review firstly introduces the classical and widely used configurations and corresponding energy-storage mechanism in detail for SICs. Then, recent progress on carbonaceous electrode materials, including cathode and anode materials, are summarized. Finally, the challenges and some suggestions on the future development of carbon-based SICs are proposed.

1. Introduction

Modern society put forward higher requirements for electrochemical energy storage (EES) systems in many fields, particularly for electric vehicles, portable electronics, and grid-level energy storage.^[1–3] Lithium-ion batteries (LIBs) and supercapacitors (SCs) have currently become the primary choices for EES devices in virtue of their outstanding overall performance.^[4–5] LIBs, as a rechargeable battery working through the intercalation/deintercalation of Li^+ ions between the negative and positive electrodes, were initially commercialized by Sony in the 1990s.^[6] The bulk electrochemical reactions for LIBs lead to a high energy density ($150\text{--}250 \text{ Wh kg}^{-1}$). However, the sluggish kinetic process of LIBs limits their power density (< 1000 W kg^{-1}) and cycling stability (< 4000 cycles).^[7] In contrast, traditional electrochemical double-layer capacitors (EDLCs) can display superior power density (> 10 kW kg^{-1}) and long-term cyclic stability (> 100,000 cycles) in non-aqueous electrolytes owing to fast-physical adsorption/desorption on the electrode/electrolyte interface. Unfortunately, the low energy density (5–10 Wh kg^{-1}) of EDLCs restricts their further application.^[8] In short, neither LIBs nor SCs can simultaneously meet further requirements with high energy-power density and excellent cycling stability. To overcome this difficulty, researchers have proposed a novel hybrid device, lithium-ion capacitors (or lithium-ion hybrid capacitors, LICs), which conquer the limitation of typical LIBs and SCs.^[9] The LICs simultaneously present the high energy-power properties and, as a result, achieve a trade-off between LIBs and SCs. The attractive LICs, constructed with the battery-type anode of LIBs and the capacitive cathode of SCs in electrolytes containing a Li-salt, exhibit a combinative working mechanism of LIBs and SCs.^[10] The hybrid working mechanism inherited from LIBs and SCs guarantees the realization of the high energy density and power density for LICs, and the LICs are thus attracting great research attention.^[8]

[a] B. Wang, X. Gao, L. Xu, K. Zou, P. Cai, X. Deng, L. Yang, Prof. H. Hou, Prof. G. Zou, Prof. X. Ji
College of Chemistry and Chemical Engineering
Central South University
Changsha 410083, P. R. China
E-mail: gq-zou@csu.edu.cn

An invited contribution to a Special Collection dedicated to Metal-Ion Hybrid Supercapacitors

The 2001 year has witnessed the birth of the first lithium-ion capacitor composed of an activated carbon (AC) cathode and a nanostructured $\text{Li}_4\text{Ti}_5\text{O}_{12}$ anode in an organic electrolyte of LIBs.^[11] The $\text{Li}_4\text{Ti}_5\text{O}_{12}$ -AC cell exhibited a high energy density of over 20 Wh kg^{-1} , preliminarily demonstrating the excellent electrochemical properties of LICs. Given this, much attention (e.g. MnO , Fe_2O_3 , TiO_2 , graphite, etc.) has been paid on developing LICs as promising alternative energy storage devices.^[7,12] At the same time, sodium-based devices are gaining special interests in view of the ever-increasing price of lithium salts and unevenly geographical distribution of lithium reserves as well as the low concentration of lithium element in the crust (~0.0017 weight%).^[13] Compared with Li in nature, indeed, Na (Figure 1a) is approximately 1300 times more than Li, and thus holds the key to the development of large-scale electrochemical energy storage devices.^[14] Notably, the research on sodium-ion batteries (SIBs) began blooming again in 2012.^[15] Meanwhile, sodium-ion capacitors (or sodium-ion hybrid capacitors, SICs) came into view for the first time. So far, SICs have already grown into a competitor for SIBs and have become the most promising candidates for next-generation energy storage devices.^[16–17] The Ragone plot presented in Figure 1c shows the current energy-power density for several efficient and important energy storage devices (i.e., LIBs, SIBs, SCs, LICs, and SICs).^[18] It should be noted that the energy-power density of SICs, which lies in between LIBs and SCs, needs to be improved. Moreover, compared with LICs, SICs (Figure 1b) possess a much higher standard redox potential (-2.71 V for Na/Na^+ vs -3.04 V for Li/Li^+),^[19] indicating that SICs may have a lower energy density in theory.^[20]

Although SICs have witnessed a rapid progress in recent years, there are still crucial tasks for further improvement, including poor rate capability of battery-type anodes, low capacity of capacitive cathodes, and the kinetic match between anodes and cathodes. Additionally, the practical feasibility of pre-sodiation strategies for SICs should be considered as well. To address the above-mentioned problems above, carbon-based materials are selected as the anode and/or cathode for SICs, owing to the advantages of low cost, sustainability, nontoxicity, abundant allotropes, and excellent physical/chemical stability.^[21–22] Among carbonaceous electrodes of SICs, the key of anode lies in improving the rate capability with sufficient capacity, which is associated with the power density of SICs. On the contrary, the crucial point of cathode is to enhance the

capacity based on superior rate capability, which can boost the energy density of SICs.

Herein, this review article (Figure 2) focuses on the latest advances in carbon-based electrode materials that act as either anode or cathode for SICs. Firstly, the classical and widely used cell configurations and the energy storage mechanism for SICs will be introduced in details. Then, the recent progress on carbonaceous electrode materials including cathode and anode materials will be summarized. Finally, the challenges and perspectives for SICs will be proposed.

1.1. Configuration and Mechanism of Sodium-Ion Capacitors

The concept of SIC has been initially explored and demonstrated in 2012 by Yin et al. (a full cell using a $\text{Na}_2\text{Ti}_3\text{O}_7$ as the anode)^[23] and Chen et al. (a full cell using V_2O_5 /carbon nanotubes composite as the anode)^[24]. Nevertheless, the possibility of a novel sodium-ion capacitor constructed by carbonaceous anode and cathode needs to be clearly proved. Fortunately, not long after, Kuratanni and co-workers^[25] reported the first dual-carbon sodium-ion capacitor consisted of a hard carbon anode and activated carbon cathode in an organic electrolyte, which shows preliminarily an important configuration of SICs. It



Baowei Wang is a master candidate of College of Chemistry and Chemical Engineering, Central South University (China). He received his B.S. degree from China University of Mining and Technology in 2019. His research interests focus on the development of advanced carbon materials for sodium-ion capacitors.



Xu Gao received his Bachelor (2015) and Master (2018) degree in Materials Science and Engineering at Sichuan University (China). He is now pursuing his Ph.D. degree at College of Chemistry and Chemical Engineering, Central South University (China). His research focuses on the energy storage materials and devices.



Laiqiang Xu is currently a PhD candidate under the guidance of Prof. Xiaobo Ji at the College of Chemistry and Chemical Engineering, Central South University (China). He received his Master degree from Shanghai University (China) in 2017. His research interests focus on the synthesis and application of solid electrolytes for rechargeable batteries.



Kangyu Zou is a Ph.D. candidate at the College of Chemistry and Chemical Engineering, Central South University (China). He received his B.Sc. and M.Sc. degrees at Northwest University (Xi'an, China) in 2015 and 2018, respectively. His research is focused on the construction of high-performance metal ion capacitors.



Peng Cai is a master candidate of College of Chemistry and Chemical Engineering, Central South University (China). He received his B.S. degree from Huazhong Agricultural University (China) in 2018. His research interests focus on the development of carbon materials for metal-ion hybrid capacitors.



Xinglan Deng is a master candidate of College of Chemistry and Chemical Engineering, Central South University (China). She received her B.S. degree from Xiangtan University (China) in 2019. Her research is focused on the development of novel electrode materials for sodium-ion capacitors.



Li Yang is a master's candidate of College of Chemistry and Chemical Engineering, Central South University (China). He received his B.S. degree from China University of Mining and Technology in 2019. His research interests focus on cathode material of lithium battery.



Hongshuai Hou is an Associate Professor at the College of Chemistry and Chemical Engineering, Central South University (China). He received his Ph.D. at Central South University (China) in 2016. His current research interests are electrochemistry and key materials for electrochemical energy storage devices.



Guoqiang Zou is an Associate Professor at the College of Chemistry and Chemical Engineering, Central South University (China). He received his Ph.D. from Central South University (China) in 2018. His current research interests are electrochemistry and key materials for electrochemical energy storage devices.



Xiaobo Ji is a "Shenghua" Professor at Central South University (China) and a Fellow of the Royal Society of Chemistry, specializing in the research and development of batteries and supercapacitor materials and their systems. He received his PhD for Electrochemistry in 2007 under the supervision of Prof. Richard Compton at the University of Oxford (UK) and undertook postdoctoral work at MIT (USA) with Prof. Donald Sadoway.

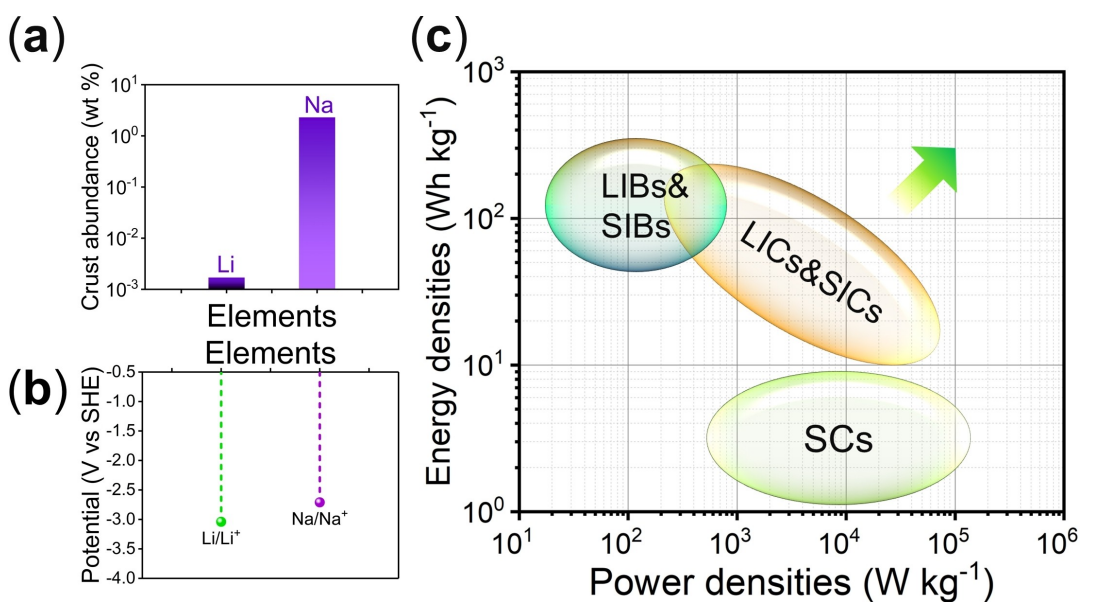


Figure 1. a) Abundance of Li and Na in the crust. b) The comparison of Li and Na in terms of standard redox potential (vs standard hydrogen electrode, SHE). c) Comparison of typical energy density and power density for lithium-ion batteries (LIBs), sodium-ion batteries (SIBs), lithium-ion capacitors (LICs), sodium-ion capacitors (SICs) and supercapacitors (SCs).

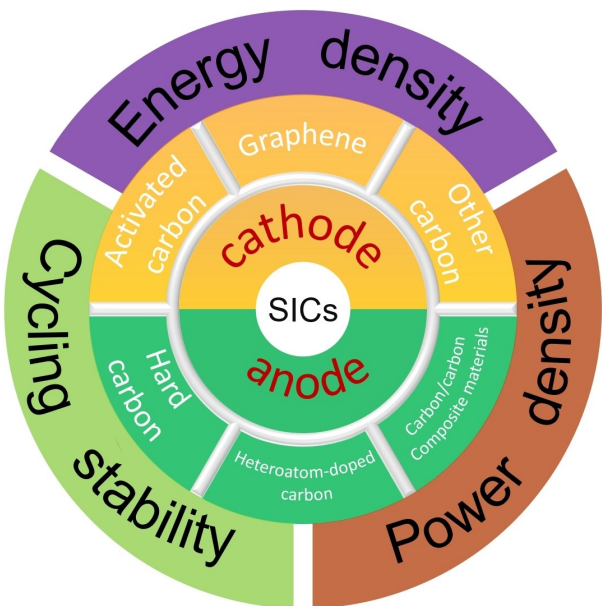


Figure 2. Schematic illustration of carbonaceous electrodes design to enhance the electrochemical properties of SICs.

is noteworthy that the configuration of SICs determines the energy storage mechanism. As a consequence, it is very necessary to confirm the configuration of SICs to understand the energy storage mechanism. Generally, SICs are composed of a capacitive electrode, battery-type electrode, separator, and electrolyte.^[26] The capacitive electrode can be used as either an anode or cathode with a battery-type counter electrode. For this reason, SICs can mainly be classified into two types.^[27] One configuration is that capacitive materials act as a cathode with high working voltage and battery-type materials serve as anode

with low working voltage, which is the most commonly used type (Figure 3a). On the contrary, the other type consists of a capacitive anode and a battery-type cathode. However, it is beyond the scope of this review to give an elaborate summary of these two configurations of SICs. In this review, we will focus on the first classical and widely used configuration.

As a hybrid device, SICs involve two kinds of energy storage mechanisms, which are closely associated with SIBs and SCs.^[28] The capacitive cathode, such as activated carbons, stores charge via electric double-layer across an electrode/electrolyte interface, corresponding to physical adsorption or non-Faradaic reaction. To increase the capacity of the capacitive cathode, pseudocapacitive materials, which can undergo a fast Faradaic reaction on the surface or near-surface of electrodes, have been used as the cathode.^[29] As for the battery-type anode, Faradaic reaction, such as the intercalation reaction, occurs in the bulk of electrode materials, which usually shows slow kinetics.^[30] Specifically, for the system using activated carbon and hard carbon as cathode and anode (Figure 3a), anions are adsorbed on the surface of AC when charging. Meanwhile, Na⁺ ions are inserted into a pre-sodiated hard carbon electrode at low operating voltage. In contrast, opposite reactions occur during the discharge process. Benefited from such a hybrid energy storage mechanism, SICs can achieve a high energy-power performance.

Energy density and power density are two important features for SICs. The energy density of SICs that we commonly use means the total stored energy per unit of weight (Wh kg⁻¹) or the total stored energy per unit of volume (Wh L⁻¹), which is usually obtained from a galvanostatic charge-discharge test. Generally, the energy density can be precisely calculated by the following equation [Eq. (1)]:

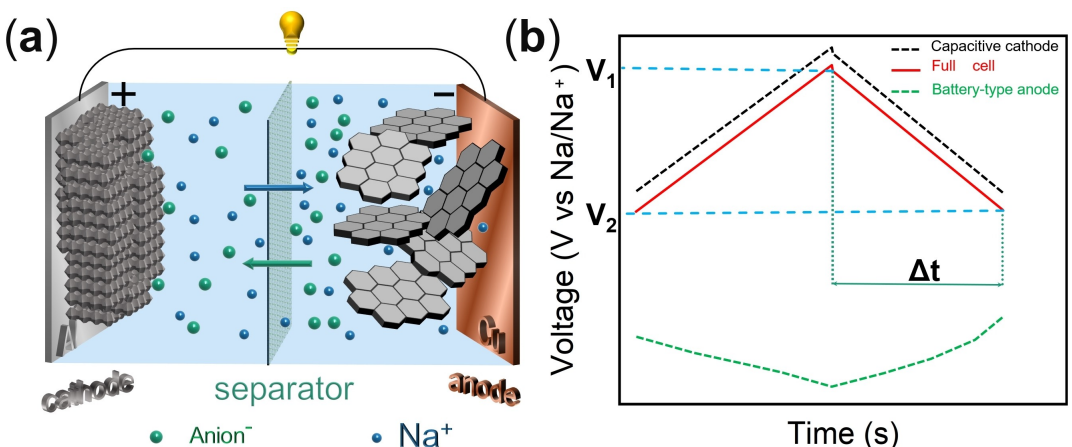


Figure 3. a) Schematic illustration of the typical configuration (cathode: activated carbon, anode: hard carbon) and b) charge-discharge curves of SICs.

$$E = \int I V dt \quad (1)$$

where E , I , V and t are energy density, discharge current density (A g^{-1}), voltage, and discharging time, respectively.

As shown in Figure 3b, owing to the approximately linear characteristic of the charge-discharge profiles, the energy density of SICs can be calculated according to the following equation [Eq. (2)]:

$$E = I \Delta t (V_1 + V_2)/2 \quad (2)$$

where E , I , and Δt are energy density, discharge current density and discharging time, and V_1 and V_2 is the maximum voltage after voltage drop and the minimum voltage, respectively. It should be noted that the Equation (2) can only be applied for the case of good linearity. In contrast, Equation (1) is a more general equation and can be applied to linear or nonlinear charge-discharge profiles.

The power density, which means how fast the energy can be released from SICs, can be commonly calculated as follows [Eq. (3)]:

$$P = E/\Delta t \quad (3)$$

here, E and Δt are the energy density and discharging time, respectively.

As an increasing number of materials (i.e., transition-metal oxides, hydroxides, sulfides, carbons, etc.) are designed into various forms of nanostructures, the electrochemical behaviors of electrode materials are neither purely capacitive nor purely Faradaic.^[31] In fact, the capacitive behaviors and Faradaic behaviors can commonly contribute the capacity simultaneously, which is extremely important for SICs. Furthermore, the advanced electrode materials of SICs is expected that battery-type anode materials can involve partially capacitive behavior and, at the same time, capacitive cathode materials can contain partially Faradaic reaction. The aim of using capacitive and Faradaic behaviors is to improve the cathode capacity and

anode rate capability, which finally increases the energy-power performance of SICs. For this reason, it is important that how we can determine the contribution of capacitive and Faradaic behaviors. Generally, the capacitive and Faradaic contribution can be qualitatively demonstrated from cyclic voltammograms according to the following power-law relationship [Eq. (4)]:

$$i = a\nu^b \quad (4)$$

where, i and ν are the current and sweep rate, and a and b are adjustable parameters.

The value of b calculated by plotting $\log(i)$ versus $\log(\nu)$ presents the extent of dominance of capacitive and Faradaic processes. The value of b equals 0.5 for the diffusion-controlled battery process, while the value of b equals 1.0 related to the capacitive process. In most cases, b ranging from 0.5 to 1.0 shows a hybrid process and demonstrates the dominant behavior according to the extent of approaching 0.5 or 1.0.

For further understanding the contribution of capacitive and Faradaic process, it is necessary to calculate quantitatively the contribution of capacitive and Faradaic behaviors according to the following equation [Eq. (5)]:

$$i(V) = k_1\nu + k_2\nu^{1/2} \quad (5)$$

where k_1 and k_2 are parameters at a given potential.

Experimentally, the data of i versus ν at a given potential is collected from cyclic voltammetry (CV) with varied scan rates. In terms of data analysis, k_1 and k_2 are calculated from a linear plot of $i/\nu^{1/2}$ versus $\nu^{1/2}$.

2. Materials for Sodium-Ion Capacitors

2.1. Cathode Materials

Mastering the design of high-capacity cathode materials is a key challenge for high-performance SICs. To address this issue, activated carbons and graphene are selected as a capacitive

cathode for SICs. The key characteristics of these cathodes will be described in this section. In addition, a novel capacitive cathode of hard carbon will also be presented to show the trend of novel capacitive cathodes for SICs.

2.1.1. Activated Carbons

ACs are the most important and commonly used cathode materials for SICs because of the merits of low cost, nontoxicity, high electrical conductivity, high specific surface area (SSA, up to $3000 \text{ m}^2 \text{ g}^{-1}$), abundant pore structure, chemical stability, and wide operation potential window.^[32] ACs can commonly be prepared from various precursors such as a polymer, biomass, coal, metal-organic framework, and organic salt.^[33] The typical potential window of ACs ranges from 1.5 to 4.2 V versus Na/Na⁺. Also, the specific capacity of commercial ACs is in the value ranges of $30\text{--}50 \text{ mAh g}^{-1}$.^[15,34] Obviously, the specific capacity of ACs is insufficient and this is the reason why the mass and thickness of ACs relative to the battery-type electrode is oversized to achieve the charge balance. It is noteworthy that the rational design of pore properties (pore volume, SSA, and pore size distribution) and the surface modification of functional groups have demonstrated valid strategies for increasing the specific capacity of ACs electrode. The pores in ACs are generally classified into three types^[35]: (i) micropores ($< 2 \text{ nm}$), (ii) mesopores (2–50 nm), and (iii) macropores ($> 50 \text{ nm}$).

The micropores accommodate ions to harvest the capacity. Also, mesopores and macropores can shorten the ion transport path to facilitate the mass transfer, leading to high rate capability. In addition to the surface rational design of pores, surface-functionalized ACs can exhibit enhanced the chemical binding with Na⁺, which is helpful to improve the specific capacity.

By constructing a hierarchical porous structure, the advantages of ACs in energy storage can be adequately utilized. Xu and co-workers^[36] demonstrated that the hierarchical porous structure with abundant mesopores, high SSA, and large pore volume plays an important role in satisfying the demand for high-rate and high-capacity ACs. As shown in Figure 4, Li and co-workers^[37] prepared a zeolitic imidazolate frameworks-8-derived porous carbon (ZDPC), which can deliver a high specific capacity of 151.7 and 96.1 mAh g^{-1} at 0.1 and 10 Ag^{-1} , respectively. Furthermore, 87% capacity retention of the ZDPC cathode electrode was gained at 1 Ag^{-1} for 2000 cycles under the voltage window of 1.5–4.0 V, showing excellent cycling stability. It is important to note that the reversible capacity of ZDPC is much larger than that of commercial ACs mentioned above. The excellent electrochemical performance is attributed to the extremely high SSA ($3738 \text{ m}^2 \text{ g}^{-1}$), large pore volume ($2.58 \text{ cm}^3 \text{ g}^{-1}$), and mesopores (2–5 nm). The surface modification of functional groups is another strategy improving the capacity of ACs. Ding and co-workers^[16] demonstrated the highly oxygen-doped functional groups (C=O quinone groups)

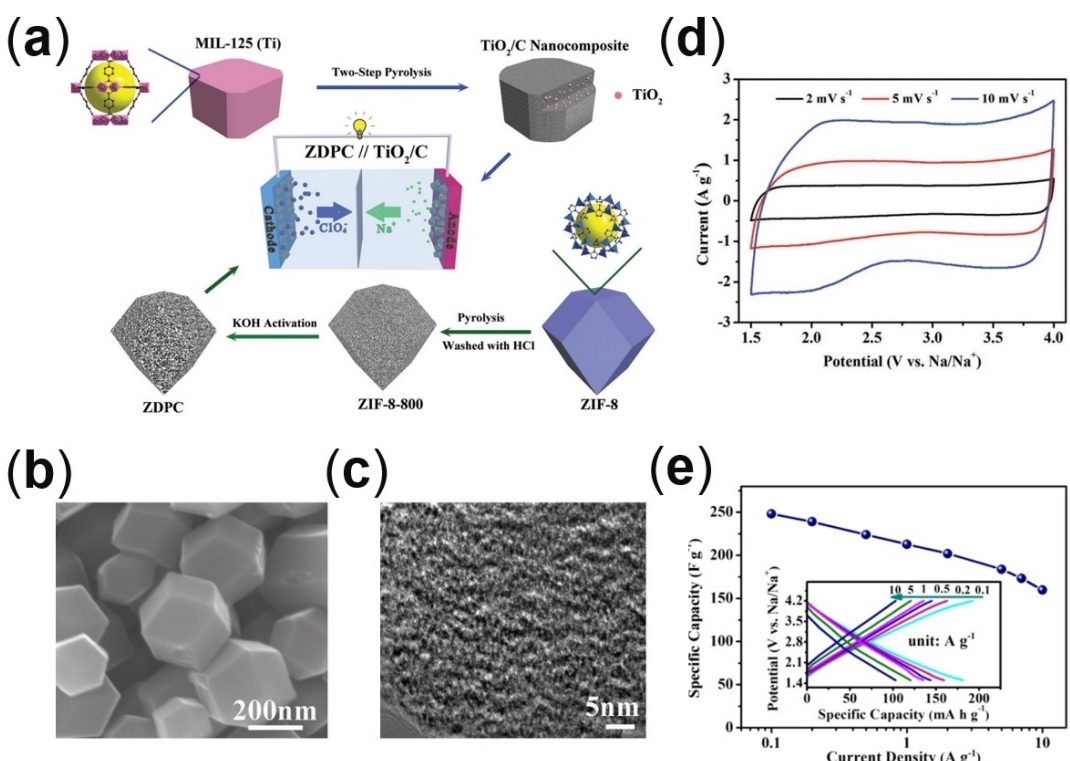


Figure 4. A zeolitic imidazolate frameworks-8-derived porous carbon (ZDPC) capacitive cathode for SICs. a) Schematic illustrations of the synthesis processes. b) Scanning electron microscopy (SEM) image. c) High-resolution transmission electron microscopy (TEM) image. d) Typical CV profiles at scan rates of 2, 5, and 10 mVs^{-1} , respectively. e) Rate performance at different current densities ranging from 0.1 to 10 Ag^{-1} (inset: charge-discharge profiles). Reproduced with permission.^[37] Copyright 2018, Wiley-VCH.

showed a superior capacity for the cathode electrode, owing to the pseudocapacitive reaction.

2.1.2. Graphene

Graphene, a well-known two-dimensional (2D) material consisting of carbon atoms in a hexagonal lattice, has captured ever-increasing attention since 2004, benefiting from exceptionally high strength, large theoretical specific surface area ($\sim 2630 \text{ m}^2 \text{ g}^{-1}$), stable chemical property, and high intrinsic electrical conductivity ($\sim 15000 \text{ cm}^2 \text{ V}^{-1} \text{ S}^{-1}$).^[38] The key features that we most value in energy-storage systems are the electrical conductivity and specific surface area. Common preparation methods for graphene include mechanical exfoliation, bottom-up synthesis, epitaxial growth, liquid-phase exfoliation, and reduction of graphene oxide.^[39] Experimentally, the most common approach to prepare graphene in energy-storage systems is the reduction of graphene oxide (GO) because of the high yield. GO is prepared by oxidizing graphite and therefore contains abundant surface functional groups (e.g., hydroxy, carboxyl, carbonyl, etc.), resulting in inferior electrical conductivity.^[40] Alternatively, owing to the weak chemical binding between Na and graphene,^[41] graphene commonly presents a low specific capacity (40–50 mAh g^{-1}) toward being

the cathode for SICs and surface modification of graphene such as heteroatom doping thus plays a key role for graphene-based cathode.^[42–43] In order to realize better electrochemical performance with high capacity and excellent rate performance for the graphene-based cathode, GO as a precursor needs to be reduced to gain reduced graphene oxide (rGO). The reduction of GO is a key step for practical graphene-based electrode, which can not only gain higher electrical conductivity but also implement directly the surface modification to offer pseudocapacitance. In addition to surface modification, the elaborate design of the graphene structure is also good support for enhancing electron transfer and mass transfer.

The surface modification has been explored by Shao et al.,^[29] Zhang et al.,^[40] Dong et al.^[44] As shown in Figure 5, Dong and co-workers^[44] demonstrated surface oxygen functional groups within the rGO and crumpled structures are favorable for the high-capacity cathode. The oxygen-functionalized crumpled graphene (OCG) electrode delivered a superior capacity of 105 mAh g^{-1} at 0.1 A g^{-1} . Even at 1 A g^{-1} after 3000 cycles, the capacity retention of 91% was achieved. Nevertheless, the voltage window of 2.5–4.2 V restricts a further increase in capacity. Specifically, the positive electrode of OCG may not make full use of the oxygen functional groups (such as C=O) to offer pseudocapacitance. But the OCG has been a vital work to pave a way forward to the high-capacity cathode.

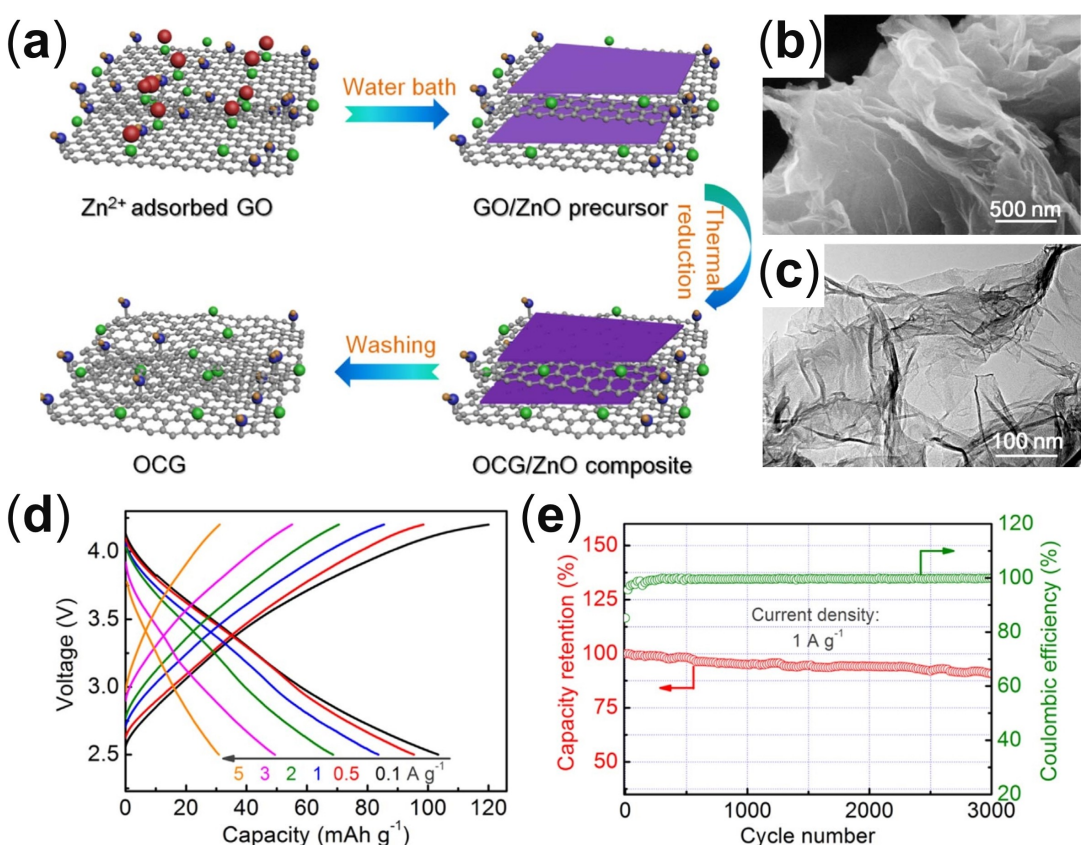


Figure 5. a) Schematic illustration of the synthesis processes for an oxygen-functionalized crumpled graphene (OCG) capacitive electrode. b) SEM image and c) TEM image of OCG. d) Charge-discharge curves at the current densities ranging from 0.1 to 5 A g^{-1} . e) The long cycling life at 1 A g^{-1} of OCG capacitive electrode. Reproduced with permission.^[44] Copyright 2017, Elsevier B.V.

For the sake of further enhancing the capacity of the graphene-based electrode, Zhang and co-workers^[42] prepared high-density porous graphene macroform (HPGM) (Figure 6a,b) integrated oxygen functional groups and folded texture by using the hydrothermal treatment and the subsequent evaporation-induced method. As shown in Figure 6c-e, HPGM exhibits sloping galvanostatic charge-discharge profiles between 1.5 and 4.0 V versus Na/Na⁺ and has a high discharge capacity of 115 mAh g⁻¹ at 0.1 A g⁻¹ after 100 cycles and ~58 mAh g⁻¹ at 1.0 A g⁻¹ after 2000 cycles, which is directly correlated with the oxygen functional groups. Even at 4 A g⁻¹, HPGM can still exhibit a specific capacity of ~80 mAh g⁻¹. The pseudocapacitive contributions are evaluated and give rise to 75.0% of the total stored charge at a scan rate of 1 mV s⁻¹. To further unveil the interplay of oxygen-containing groups and

folded structure, the controlled thermal reduction is conducted at different temperatures of 300, 400, 500, 600, and 800 °C for 2 h in an inert atmosphere, respectively. Capacitive contributions of 61.5, 56.3, 45.0, 38.9, and 33.3% at a scan rate of 1 mV s⁻¹ are obtained at different thermal reduction samples of 300, 400, 500, 600, and 800 °C, respectively, corresponding to the decrease of atomic contents oxygen measured from X-ray photoelectron spectroscopy (XPS). These results elucidate the crucial effect of oxygen functional groups and the folded structure.

Very recently, Ma and co-workers^[45] prepared a compact, oxygen-rich, and highly ordered graphene solid (HOGS) (Figure 7a,b) by using hydrothermal reduction and capillary densification with long-range ordered lamellar graphene oxide liquid crystals (LCs) as the precursor. When investigated as a

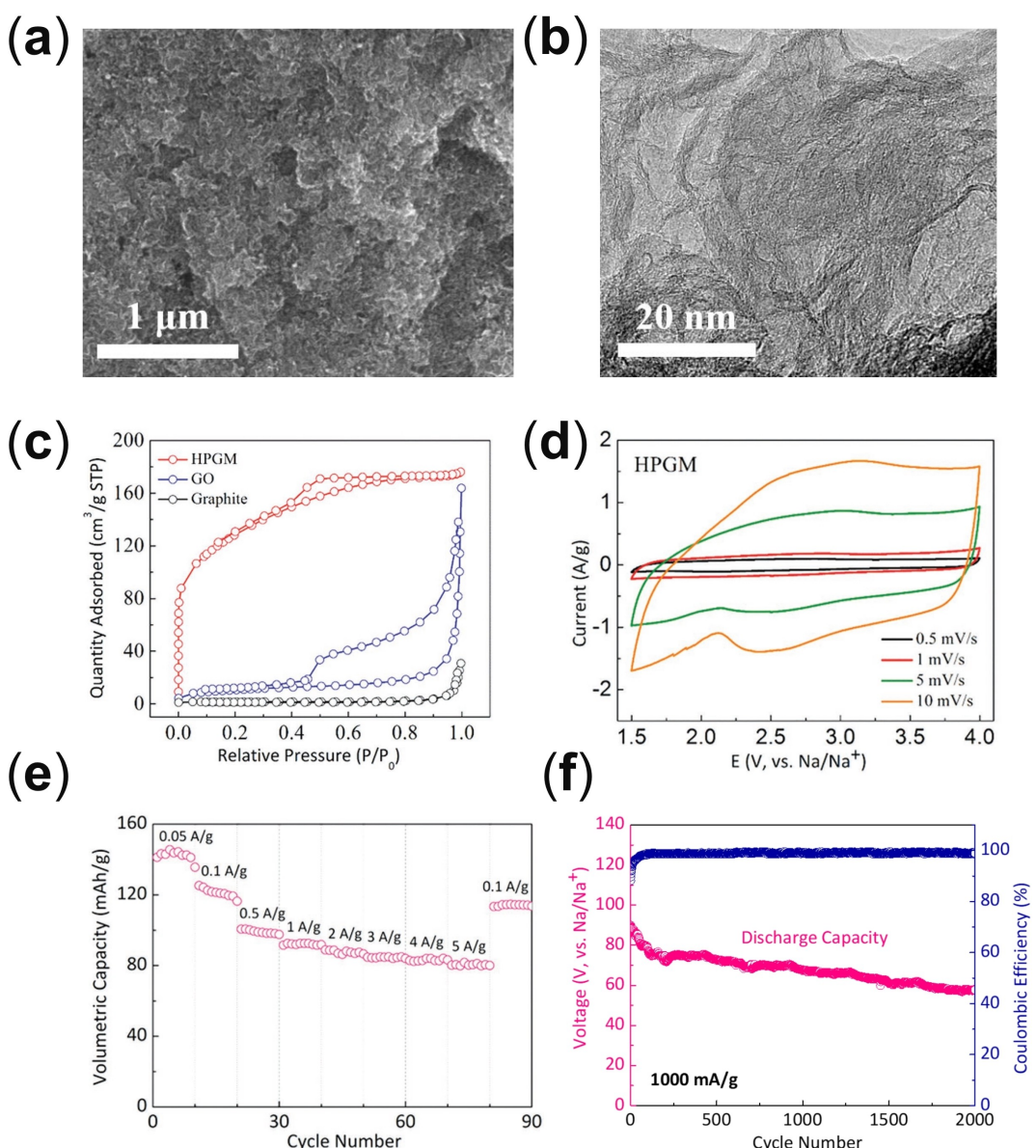


Figure 6. a) SEM image and b) TEM image of high-density porous graphene macroform (HPGM). c) N₂ adsorption isotherm for HPGM. d) CV curves of HPGM at scanning rates ranging from 0.5 to 10 mV s⁻¹. e) Rate performance at current densities ranging from 0.05 to 5 A g⁻¹ and f) cycling life at 1 A g⁻¹ for HPGM electrodes. Reproduced with permission.^[42] Copyright 2018, Wiley-VCH.

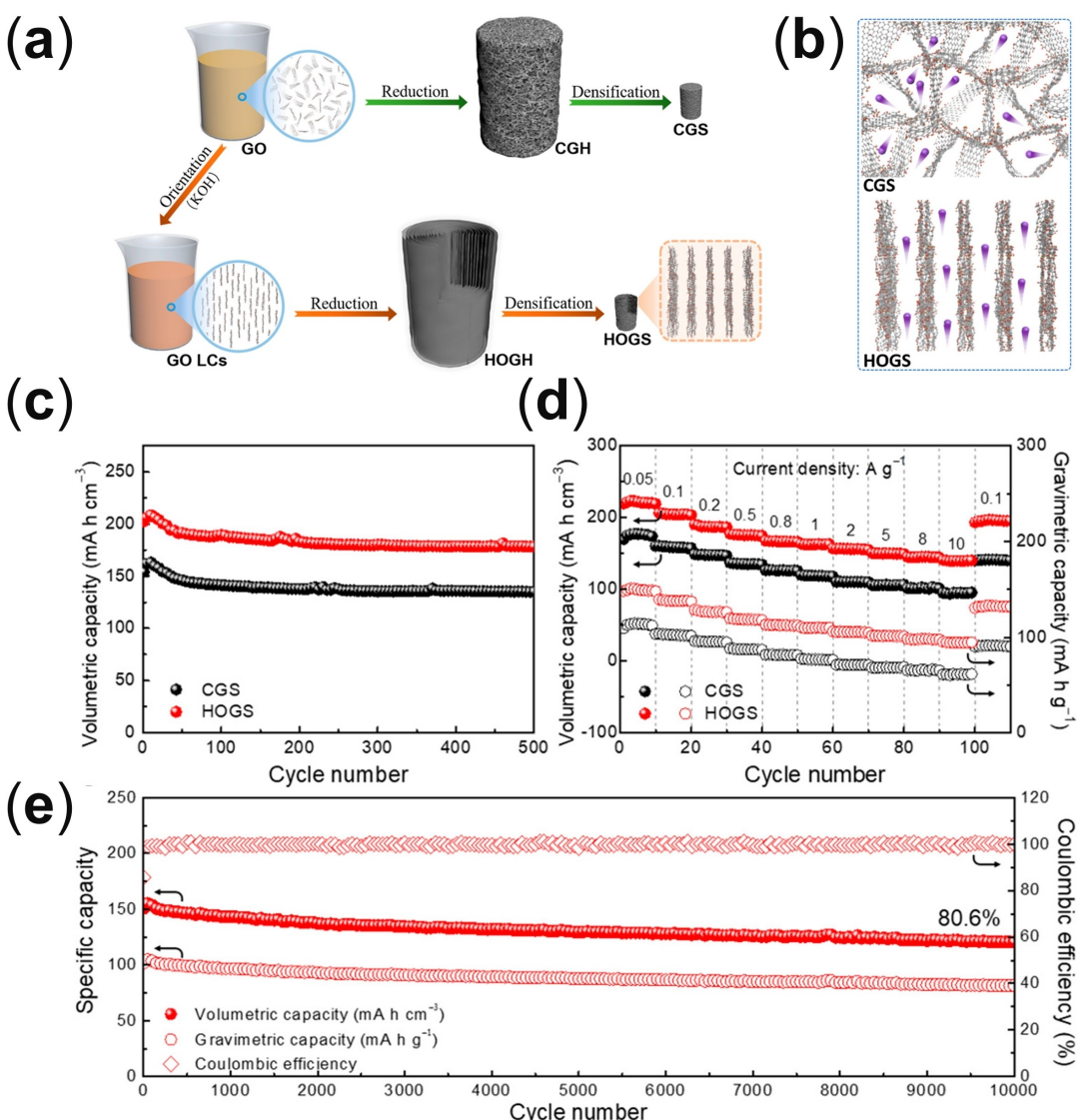


Figure 7. a) Schematic illustration of preparation of highly ordered graphene solid (HOGS) and b) the fast ion transport within HOGS. c) Cycling performance at the current density of 0.1 A g^{-1} and d) rate performance at different current densities for HOGS electrode. e) Long-term cycling performance of HOGS at a current density of 2 A g^{-1} . Reproduced with permission.^[45] Copyright 2019, American Chemical Society.

cathode material for SICs, as shown in Figure 7c-e, HOGS delivers a high volumetric capacity of 219 mAh cm^{-3} at 0.05 A g^{-1} and a superior rate capability of 139 mAh cm^{-3} (or 94 mAh g^{-1}) at 10 A g^{-1} , respectively. Even after 10000 cycles, it can still reach a capacity of 121 mAh cm^{-3} or 82 mAh g^{-1} at a current density of 2 A g^{-1} , with 80.6% capacity retention and 0.0019% fading rate per cycle. The superb volumetric energy density of 416 Wh L^{-1} at a power density of 148 W L^{-1} and the ultrahigh power density of 36200 W L^{-1} at an energy density of 253 Wh L^{-1} has been calculated by using HOGS as the cathode and assumed material as the anode. Specifically, the assumed anode material possesses the same specific capacity and loading mass with HOGS, as well as an identical operating voltage with sodium foil. The outstanding electrochemical performance exhibited by HOGS is ascribed to highly ordered structure, the high packing density of up to 1.48 g cm^{-3} , and high SSA of $529 \text{ m}^2 \text{ g}^{-1}$, as well as abundant oxygen functional

groups of up to 18.8%. More specifically, the oxygen functional groups can offer pseudocapacitive reactions to increase capacity and high ordered structure simultaneously can facilitate ion diffusion.

These studies suggest that the porosity and oxygen functional groups play key roles in affecting the capacitive behavior of graphene-based cathodes. However, other functional groups for SICs are rarely reported, and further research is needed. Specially, to deepen the understanding, density functional theory calculations for the electrochemical reaction are also needed.

2.1.3. Other Carbon-Based Cathode Materials

In addition to AC and graphene, all researchers are also aiming at developing novel capacitive cathode for SICs to meet the

requirements of the future generation of electronic devices. Hard carbon, a well-known negative electrode for sodium-ion batteries, is beginning to be tentatively explored as a capacitive cathode.^[46–47] For example, as shown in Figure 8, Chen and co-workers^[46] prepared a nitrogen-doped microporous hard carbon (NPHC) via the pyrolysis of chemosynthetic polypyrrole soaked with ZnCl₂ using the commercial pyrrole monomer as a precursor. The NPHC exhibits quasilinear galvanostatic charge-discharge curves between 1.0 and 4.7 V versus Na/Na⁺ as the capacitive cathode for SICs, which is different from previous

reports. It exhibits a reversible capacity of 197, 141, and 68 mAh g⁻¹ at the current density of 1.0, 2.0, 5.0 Ag⁻¹, respectively. In this electrode, the cycling stability with a capacity of 100 mAh g⁻¹ after 1000 cycles at 2.0 Ag⁻¹ is obtained. It is worth noting that the superior electrochemical performance is attributed to defects probed by the I_D/I_G ratio of 1.1, the high specific surface area of ~700 m² g⁻¹, and predominant micropores. When coupled with a soft carbon anode, the obtained full cell, with the voltage window of 0–4.7 V versus Na/Na⁺, shows a high energy density of

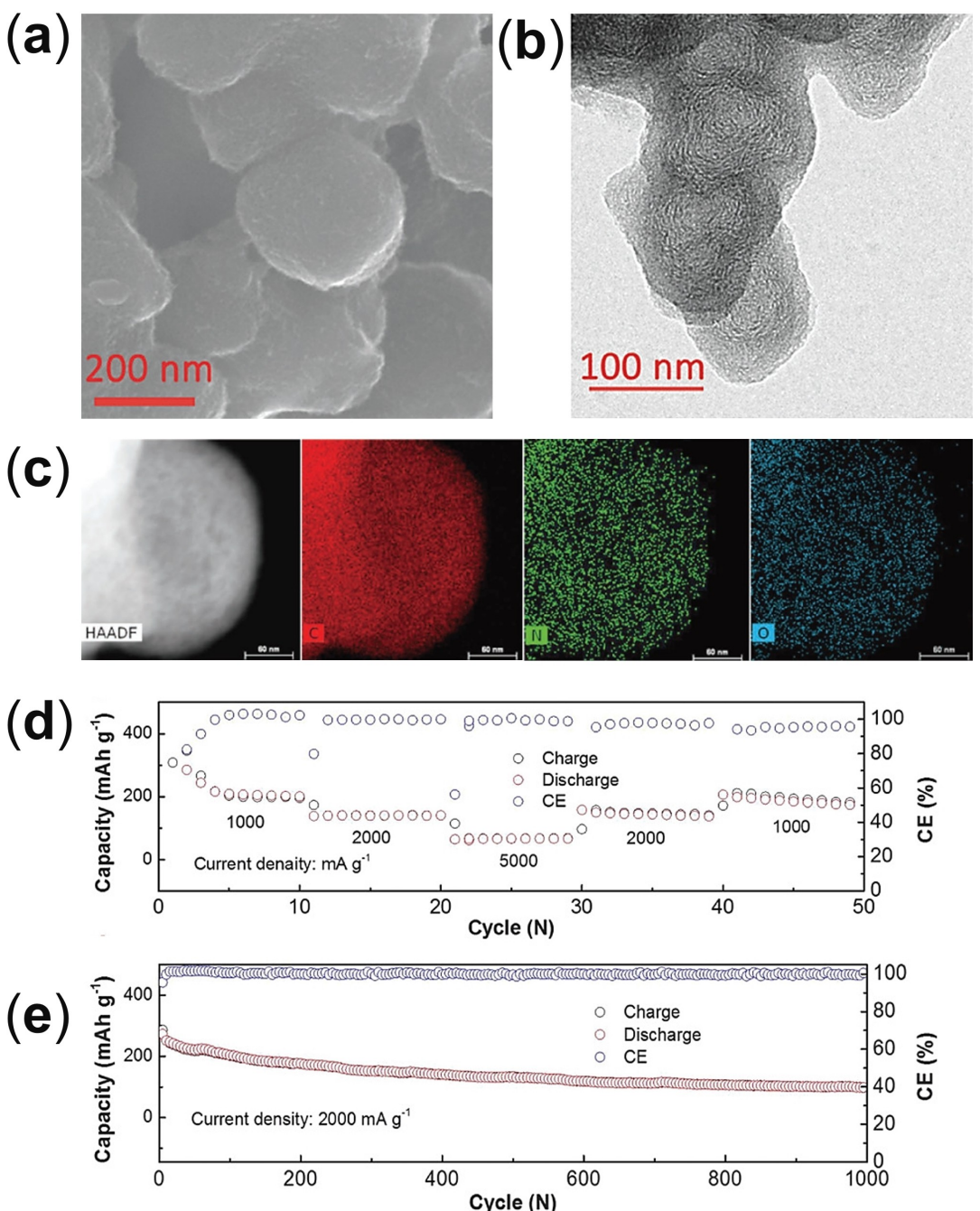


Figure 8. a) SEM image. b) TEM image. c) Elemental mapping (scale bar: 60 nm). d) Rate performance of a nitrogen-doped microporous hard carbon (NPHC) at different current densities. e) Cycling stability at the current density of 2 Ag⁻¹ for NPHC electrode. Reproduced with permission.^[46] Copyright 2018, Wiley-VCH.

245.7 Wh kg⁻¹ at 1626 W kg⁻¹ and a high power density of 13846.1 W kg⁻¹ at 50 Wh kg⁻¹. The hard carbon opens a new avenue for the high-capacity capacitive cathode. Another anode material (soft carbon) with sloping galvanostatic charge-discharge profiles over 1.0 V may be utilized as a capacitive cathode and help achieve the practical applications for SICs.

2.2. Anode Materials

As an important component, anode materials play a key role in achieving high energy-power performance SICs. Generally, suitable anode materials for SICs need to possess high capacity under low voltage window (<1.0 V vs Na/Na⁺) and excellent rate capability, as well as superior cycling stability.^[48] Benefiting from low cost, sustainability, and good physical/chemical stability, a series of carbonaceous materials such as hard carbon, heteroatom-doped carbon, and carbon/carbon composite are commonly selected as the battery-type anode in electrochemical energy storage devices, which will be illustrated in this section. The relationship between carbonaceous materials properties and its electrochemical performance will be presented, which will help to understand the rational design of carbonaceous materials.

2.2.1. Hard Carbon

Theoretical calculations and experiments have demonstrated that the ability of sodium storage in graphite is rather poor. The low specific capacity (~35 mAh g⁻¹) restricts its application in sodium-based energy storage systems.^[41] In contrast, hard carbon, a well-known amorphous carbon material containing graphite-like microcrystallites and amorphous region, commonly has a high capacity and consequently attracts tremendous focuses and research.^[49] To improve the electrochemical performance of hard carbon, the structure (e.g., large interlayer distance, etc.), abundant defects (e.g., edges, vacancies, etc.), micropores (open pores and closed pores), and foreign atoms (e.g., N, S, P, etc.) are introduced to hard carbon.^[50] For example, Kubota and co-workers^[50] demonstrated that the structure and defects in hard carbon significantly influenced its electrochemical performance. Abundant defects will enhance chemical bonding between Na and hard carbon. Meanwhile, vast defects will also lead to low initial Coulombic efficiency (ICE). In short, optimizing the properties of hard carbon is a key challenge for developing the high-performance anode. The most common preparation strategy for hard carbon is the pyrolysis of polymer, biomass, and small organic molecules in an inert atmosphere.^[33] The galvanostatic charge-discharge curves in hard carbon are generally into two regions: (i) high-potential sloping region (>0.1 V vs Na/Na⁺), (ii) low-potential plateau region (<0.1 V vs Na/Na⁺). The Na storage mechanism ("intercalation-adsorption" mechanism vs "adsorption-intercalation" mechanism) in two distinct voltage regions is still controversial.^[49–50]

Recently, Wang et al.^[51] demonstrated hard carbon was an extremely promising anode for achieving a high energy density of SICs. Aiming at high energy-power density, Ajuria and co-workers^[34] prepared a SIC using a hard carbon derived from a low-cost recycled olive pit as an anode. The SIC exhibited a high energy density of ~102 Wh kg⁻¹ and high power energy of 9000 W kg⁻¹ with the capacity retention of 90% after 1000 cycles. Because of the renewability and low cost of biomass, Liu and co-workers^[52] prepared a garlic-derived hard carbon (GDHC) as a negative electrode for SICs. When coupled with a porous carbon derived from garlic, the GDHC showed a remarkable energy density of 156 Wh kg⁻¹ at 355 W kg⁻¹.

Very recently, Xu and co-workers^[53] prepared a hard carbon derived from mulberry tree stems. As shown in Figure 9, hard carbon consisting of irregular particles delivered a high reversible capacity of ~310 mAh g⁻¹ at 0.05 A g⁻¹ and ~100 mAh g⁻¹ at 3.2 A g⁻¹, respectively. Notably, the capacity retention of 80% was obtained at the current density of 0.8 A g⁻¹ after 1000 cycles. A SIC full cell was fabricated with the hard carbon and a biomass-derived AC as the anode and cathode, which showed a high energy density of 61 Wh kg⁻¹ at a specific power of 0.1 kW kg⁻¹ and a high power output of 24 kW kg⁻¹ at a specific energy of 12 Wh kg⁻¹ with the voltage window of 1.0–4.0 V. The capacitance retention of 91.5% was gained at the current density of 1.0 A g⁻¹ after 1000 cycles.

The above examples have proved that hard carbon is a vital element for advanced sodium-ion capacitors combined with high energy density and power density. Nevertheless, the electrochemical performance of hard carbon is still sufficient for advanced SICs. As a result, exploring high-performance hard carbon anode is a major challenge for developing SICs.

2.2.2. Heteroatom-Doped Carbon Materials

Heteroatom doping (such as N, S, P, and B) in carbon materials is an extremely effective strategy to improve the electrochemical properties. In order to boost electrochemical performance, the key challenge for heteroatom-doped carbon materials lies in mastering the design of the type and concentration of doped atoms. Simultaneously, a high specific surface area in doped carbon materials is necessary. Furthermore, the reason for these designs is that heteroatom atoms offer strong chemical bonding and a high specific surface gives rise to sufficient exposure of redox-active sites.

Recently, Liao and co-workers^[54] assembled a novel SIC with an N and S co-doped hollow carbon nanofibers anode and an AC cathode. Because of the high N content of 7.01% and S content of 3.15%, the SIC delivered a high energy density of 116.4 Wh kg⁻¹ and a high power output of 20 kW kg⁻¹. Even at the current of 2.0 A g⁻¹, the SIC exhibited about 81% capacity retention after 3000 cycles in the voltage window of 0–4.0 V. Additionally, Dong and co-workers^[55] presented a simple strategy for the synthesis of nitrogen-doped porous carbon (denoted as DCDC–Na) by sodium nitrate-assisted carbonization of *k*-Carrageenan. The DCDC–Na with a high nitrogen content of 9.3 at. % and a large specific surface area of

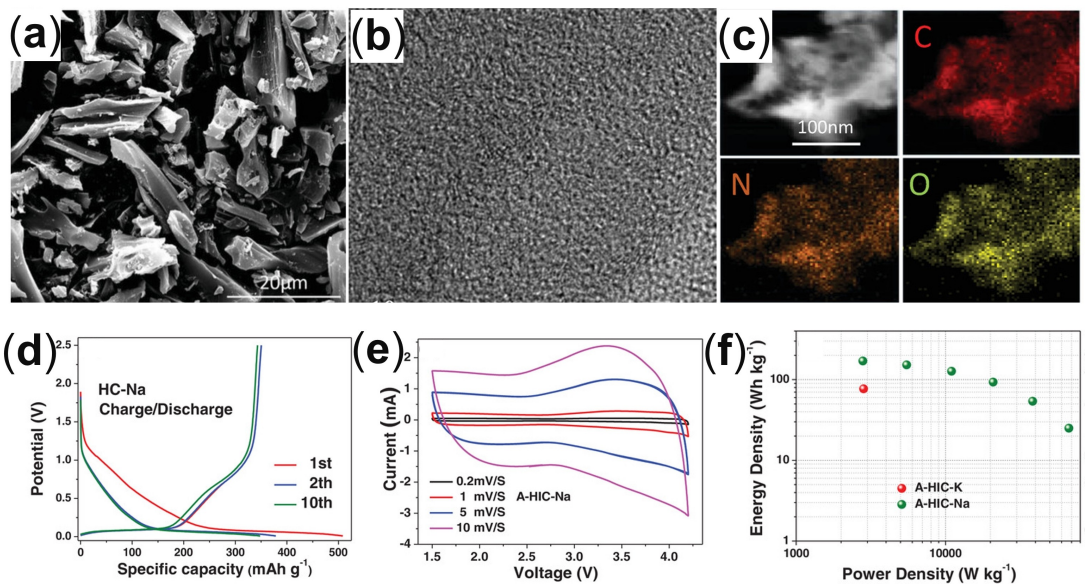


Figure 9. a) SEM image and b) high-resolution TEM image of hard carbon. c) Elemental mapping. d) Charge-discharge curves of hard carbon at a current density of 0.03 A g^{-1} . e) CV curves and f) Ragone plot for SICs. Reproduced with permission.^[53] Copyright 2019, Wiley-VCH.

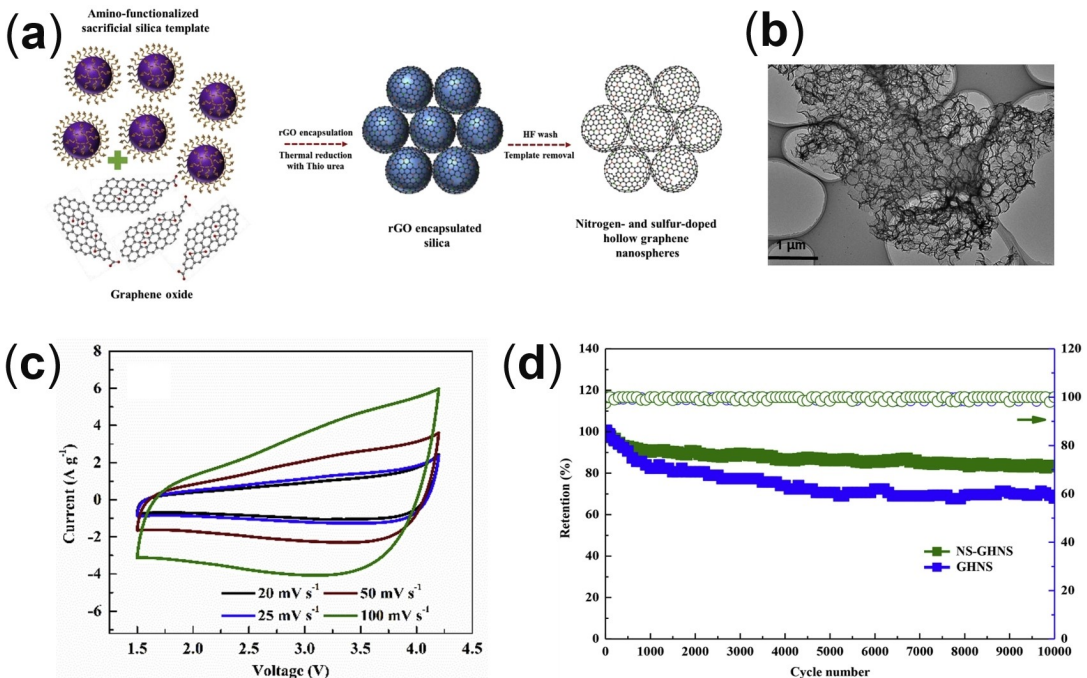


Figure 10. a) Schematic illustration of the synthesis of nitrogen and sulfur co-doped graphene hollow nanospheres (NS-GHNS) by a sacrificial template method. b) TEM image of NS-GHNS. c) CV curves and d) cycling stability at 5 A g^{-1} for the NS-GHNS//NS-GHNS cell. Reproduced with permission.^[57] Copyright 2019, Elsevier B.V.

$582 \text{ m}^2 \text{ g}^{-1}$ delivered a high specific capacity of 419 mAh g^{-1} at 50 mA g^{-1} and 131 mAh g^{-1} at 10 Ag^{-1} . SIC based on the DCDC-Na anode can exhibit an energy density of 110.8 Wh kg^{-1} and retain 85% of initial capacity after 10 000 cycles. Moreover, Yang and co-workers^[56] designed high-level nitrogen and phosphorus (12.8 at. % N and 4.1 at. % P) co-doping carbon nanofiber films (denoted as NP-CNF), which delivered 260.3 mAh g^{-1} at 0.1 Ag^{-1} . The SIC employed NP-CNF

as anode displayed a high energy density of 95.6 Wh kg^{-1} and a high power density of 20.0 kW kg^{-1} as well as outstanding cycling stability (77.8% capacity retention after 10 000 cycles at 2.0 Ag^{-1}). However, it is worth pointing out that the specific surface area of NP-CNF was $11.5 \text{ m}^2 \text{ g}^{-1}$, which may restrict the electrochemical performance of NP-CNF.

Heteroatom-doped carbon microspheres are particularly representative battery-type anode materials for SICs. As shown

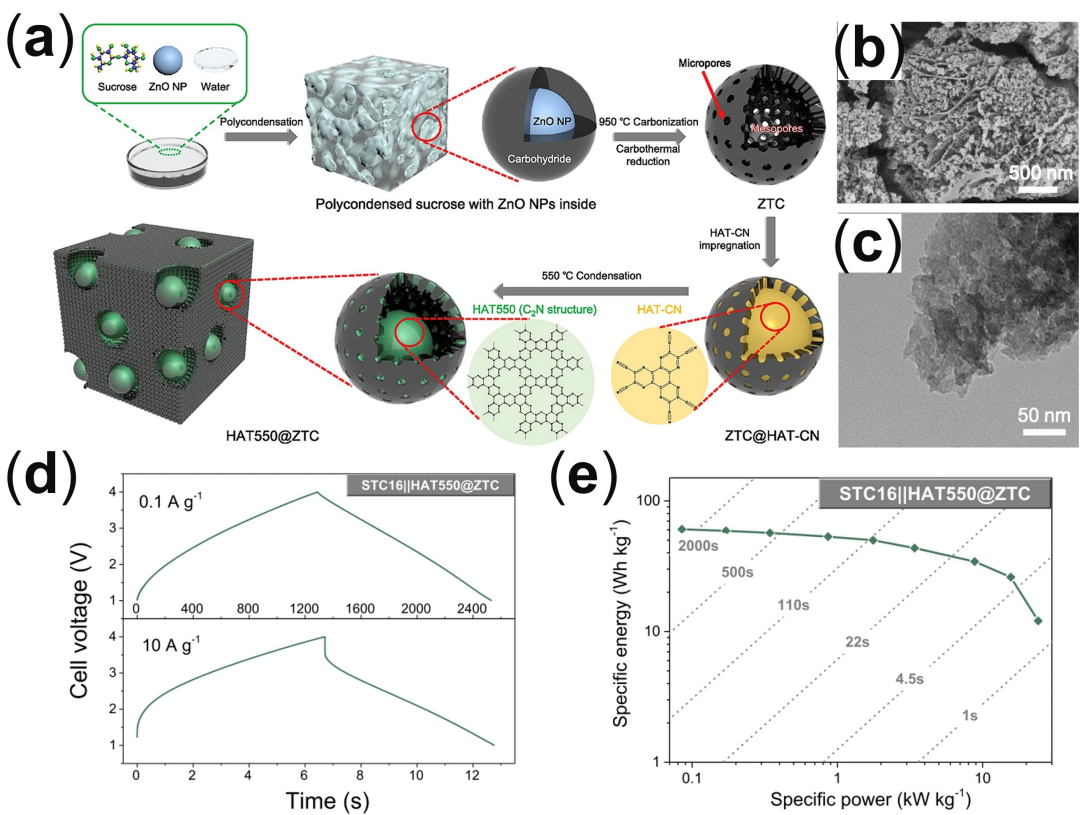


Figure 11. a) Schematic illustration of the preparation of a unique 3D nanocomposite material (HAT550@ZTC). b) SEM image and c) TEM image of HAT550@ZTC. d) Galvanostatic charge-discharge profiles at 0.1 and 10 A g⁻¹ for the full cell with HAT550@ZTC as anodes and a salt-templated carbon (STC-16) as cathodes. e) Ragone plot of the SIC full cell. Reproduced with permission.^[60] Copyright 2019, Elsevier B.V.

in Figure 10, Thangavel and co-workers^[57] synthesized nitrogen and sulfur co-doped graphene hollow nanospheres (denoted as NS-GHNS) by a facile sacrificial template method, which possessed a high specific surface area ($\sim 320 \text{ m}^2 \text{ g}^{-1}$) and high heteroatom content (3.34 at.% N and 1.82 at.% S). The discharge capacity measured at the current of 5 A g^{-1} was $\sim 141 \text{ mAh g}^{-1}$ after 10 000 cycles with a capacity retention of $\sim 86\%$, indicating the important effect of the improved electrical conductivity, high specific surface area, and ample N and S dopants. Meanwhile, computational simulations reveal that the unique hollow architecture can give rise to lower formation energies between Na and 3D hollow carbon. Interestingly, the as-built SIC using NS-GHNS as anode and cathode can deliver remarkable energy density of 121 and 69 Wh kg^{-1} at 100 and 51 kW kg^{-1} within 1.5–4.2 V, respectively, as well as superior cycling stability of 90% capacity retention over 5000 cycles.

The full utilization of the merits of superior rate capability and fast kinetic behavior (surface-controlled capacitive storage) in heteroatom-doped carbon anode strongly rely on sufficient content and different types of heteroatoms. In a word, the influence of the content and types of foreign atoms in carbonaceous materials on electrochemical properties need to deepen the understanding, in our view, and the synthesis of highly heteroatom-doped carbon materials with versatile active

sites by simple, effective, and scalable methods is still needed to explore further.

2.2.3. Carbon/Carbon Composite Materials

Fast and reversible sodium storage in functional groups plays a crucial role in the anodes of sodium ion capacitors, which was supported by density functional theory (DFT) calculations by William et al.^[41] and experimental work^[58]. Nevertheless, carbonaceous materials with a high content of functional groups such as non-graphitic nitrogen probably result in an inferior intrinsic electrical conductivity, hindering electron transfer in carbon electrodes. Constructing carbon/carbon composite materials is another possible avenue to enhance the electrochemical properties of SICs, which is consistent with the concept of “decoupling the role of electron transport and ion storage” in a single electrode by employing nano-sized two-phase composite materials as proposed by Maier et al.^[59]. In other words, ions such as Na^+ and electrons are separately stored in the same electrode composed of different phases where transport and accommodation of ions occur in one phase of a composite material, and transfer of electrons takes place in the other phase of the same composite, offering simultaneously high storage capacity and fast kinetics.

Recently, Yan and co-workers^[60] initially explored and proved the concept of “decoupling the role of electron transport and ion storage” by constructing a nano-sized composite material composed of highly nitrogen-rich carbon nanoparticles which are embedded into a remarkably electrically conductive mesoporous carbon matrix (Figure 11a-c). In the constructed nanocomposite material, the highly conductive mesoporous carbon (ZnO templated carbon, denoted as ZTC) as a matrix host nitrogen-rich carbon nanoparticles derived from a condensed hexaazatriphenylene-hexacarbonitrile (HAT-CN) precursor, thus resulting in the formation of a unique 3D nanocomposite material (denoted as HAT550@ZTC) of nitrogen-rich carbon nanoparticles within the conductive porous networks. More importantly, the nitrogen content of HAT550@ZTC is measured as high as 26 wt%, leading to a large number of nitrogen-containing functional groups. Meanwhile, the SSA and total pore volume remain $415 \text{ m}^2 \text{ g}^{-1}$ and $0.6 \text{ cm}^3 \text{ g}^{-1}$ versus ZTC ($1762 \text{ m}^2 \text{ g}^{-1}$ and $2.9 \text{ cm}^3 \text{ g}^{-1}$) to guarantee short transport length of the sodium ions. HAT550@ZTC was fabricated into electrodes for half-cell measurements in Swagelok-type test cells. The electrochemical properties of HAT550@ZTC were evaluated by galvanostatic charge-discharge profiles from 0.1 to 20 Ag^{-1} between 0 and 2.5 V versus Na/Na⁺. As expected, HAT550@ZTC exhibited high reversible capacity (343 mAhg⁻¹ at 0.1 Ag^{-1}), ultra-high rate capability (166 mAhg⁻¹ at

10 Ag^{-1}), 124 mAhg⁻¹ at 20 Ag^{-1}), and long-cycling stability (~90% capacity retention after 1300 deep charging-discharging cycles at 0.5 Ag^{-1}). To further explore the practical applicability, a full-cell sodium-ion capacitor using HAT550@ZTC as the anode and a salt-templated carbon (denoted as STC-16) as the cathode was fabricated. The HAT550@ZTC | | ATC16 cell operated between 1.0 and 4.0 V and presented sloping profiles. Calculated from the galvanostatic charge-discharge profiles, the full cell provided the maximum energy density of 61 Wh kg^{-1} at a specific power of 0.1 kW kg^{-1} and still maintained 12 Wh kg^{-1} at a specific power of 24 kW kg^{-1} (Figure 11d, e). Even after 1000 cycles at a specific current of 1.0 Ag^{-1} , 91.5% capacitance retention was measured, corresponding to ~0.008% capacitance loss per cycle. In summary, based on this composite of HAT550@ZTC, the concept of decoupling electron transport and ion storage in Na-ion capacitors was demonstrated, giving it great potential towards simultaneously realizing high energy-power properties.

SICs have been proved viable in 2012, however, it is still at the early stage when compared to the LICs. In our view, the understanding of the published literature facilitates the avenue to advanced carbon electrode for sodium-ion capacitors. The progress that we are interested in for carbon-based SICs is summarized and compared. Table 1 presents the full cell voltage window, maximum energy density, maximum power

Table 1. A summary of SIC devices based on carbon-based electrode materials.

Anode//cathode	Electrolyte	Voltage [V]	Energy density and power density	Cycling retention	Year
N/O co-doped carbon fibers// porous carbon fibers ^[36]	1.0 M NaClO ₄ in EC:PC (1:1) with 5% FEC	1.5–4.0	59.2 Wh kg^{-1} at 275 W kg^{-1} ; 38.7 Wh kg^{-1} at 5500 W kg^{-1}	48.6% after 5000 cycles; 0.5 Ag^{-1}	2020
TiO ₂ /C//hierarchical nanoporous carbon ^[37]	1.0 M NaClO ₄ in EC:PC (1:1) with 5% FEC	1.0–4.0	142.7 Wh kg^{-1} at 250 W kg^{-1} ; 61.8 Wh kg^{-1} at 25000 W kg^{-1}	90% after 10 000 cycles; 1.0 Ag^{-1}	2018
Oxygen-functionalized graphene// oxygen-functionalized graphene ^[44]	P(VDF-HFP) gel polymer electrolyte	0.5–3.5	121.3 Wh kg^{-1} at 300 W kg^{-1} ; 51.2 Wh kg^{-1} at 8000 W kg^{-1}	86.7% after 2500 cycles; 0.5 Ag^{-1}	2017
Soft carbon//N-doping porous hard carbon ^[46]	1.0 M NaPF ₆ in EC:DMC(6:4)	0.0–4.7	245.7 Wh kg^{-1} at 1626 W kg^{-1} ; 50.0 Wh kg^{-1} at $13846.1 \text{ W kg}^{-1}$	65.0% after 1000 cycles; 5.0 Ag^{-1}	2018
N-doping hard carbon // N-doping hard carbon ^[47]	1.0 M NaPF ₆ in EC:DEC(4:6)	1.0–4.7	197.0 Wh kg^{-1} at 219 W kg^{-1} ; 88.0 Wh kg^{-1} at 5468 W kg^{-1}	72.2% after 500 cycles; 5.0 Ag^{-1}	2020
Hard carbon//AC ^[34]	1.0 M NaPF ₆ in EC:PC(1:1)	1.5–4.2	100.0 Wh kg^{-1} at 28 W kg^{-1} ; 25.0 Wh kg^{-1} at 7000 W kg^{-1}	70.0% after 5000 cycles; 2.0 Ag^{-1}	2017
Hard carbon//AC ^[52]	1.0 M NaClO ₄ in EC:DEC(1:1) with 5% FEC	1.5–4.2	156.0 Wh kg^{-1} at 355 W kg^{-1} ; 31.0 Wh kg^{-1} at 38910 W kg^{-1}	73.0% after 10 000 cycles; 5.0 Ag^{-1}	2019
Hard carbon//AC ^[53]	1.0 M NaClO ₄ in EC:DEC(1:1)	1.5–4.2	170.0 Wh kg^{-1} at 2800 W kg^{-1} ; 54.0 Wh kg^{-1} at 38400 W kg^{-1}	70.0% after 10 000 cycles; 0.4 Ag^{-1}	2019
N/S co-doped hollow carbon nanofibers//AC ^[54]	1.0 M NaClO ₄ in EC:DMC(1:1) with 5% FEC	0.0–4.0	116.4 Wh kg^{-1} at 200 W kg^{-1} ; 18.2 Wh kg^{-1} at 20000 W kg^{-1}	81.0% after 3000 cycles; 2.0 Ag^{-1}	2018
N-doping carbon// methylcellulose derived carbon ^[55]	1.0 M NaClO ₄ in EC:DEC(1:1)	0.0–4.0	110.8 Wh kg^{-1} at 329 W kg^{-1} ; 40.5 Wh kg^{-1} at 12100 W kg^{-1}	85.0% after 10 000 cycles; 5.0 Ag^{-1}	2018
N/P co-doped carbon fibers//AC ^[56]	1.0 M NaClO ₄ in EC:DMC(1:1)	0.0–4.0	95.6 Wh kg^{-1} at 200 W kg^{-1} ; 10.6 Wh kg^{-1} at 20000 W kg^{-1}	77.8% after 10 000 cycles; 2.0 Ag^{-1}	2019
N/S co-doped hollow carbon spheres// N/S co-doped hollow carbon spheres ^[57]	1.0 M NaClO ₄ in EC:DEC(1:1)	1.5–4.2	121.0 Wh kg^{-1} at 100 W kg^{-1} ; 69.0 Wh kg^{-1} at 51000 W kg^{-1}	85.0% after 10 000 cycles; 5.0 Ag^{-1}	2019
N-doped carbon fibers// salt-templated carbon ^[58]	1.0 M NaClO ₄ in EC:PC:FEC (45:45:10 by mass)	0.5–4.0	95.0 Wh kg^{-1} at 190 W kg^{-1} ; 18.0 Wh kg^{-1} at 13000 W kg^{-1}	90.0% after 1000 cycles; 1.0 Ag^{-1}	2019
N-doped carbon fibers// salt-templated carbon ^[60]	1.0 M NaClO ₄ in EC:PC:FEC (45:45:10 by mass)	1.0–4.0	61.0 Wh kg^{-1} at 100 W kg^{-1} ; 12.0 Wh kg^{-1} at 24000 W kg^{-1}	91.5% after 1000 cycles; 1.0 Ag^{-1}	2019

density, and cycling retentions for the latest and representative SICs. As one can see from table 1, excellent electrochemical properties (up to 245.7 Wh kg^{-1} at a power density of 1626 W kg^{-1}) have been reported in SICs. The reported cell clearly demonstrates A great potential for being the next-generation carbon-based hybrid capacitors.

3. Conclusions and Perspectives

In summary, SICs have emerged as novel devices for next-generation energy storage systems benefiting from the high energy-power properties and the high concentration of Na in the crust. This review summarizes the latest advances of carbonaceous electrode materials as the anode and cathode for SICs. As shown in Figure 12, the capacitive cathode materials focus on ACs, graphene, and other carbon cathode materials. As for the battery-type anode materials (Figure 12), hard carbon, heteroatom-doped carbon, and carbon/carbon composites are highlighted.

As the most promising electrode candidate for SICs, carbonaceous materials still face great challenges in overcoming the scientific issues of kinetic mismatch and capacity balancing. Note that enhancing the electrochemical performance for SICs needs the overall consideration. As it follows from the published literature, the battery-type anode materials

require the key properties of the high capacity under relatively low potential ($< 1.0 \text{ V vs Na/Na}^+$), outstanding rate capability, and a long lifespan. As for the capacitive cathode materials, it is clear that improving the specific capacity is the most crucial mission. Moreover, the pre-sodiation of electrode materials is an important issue as well. Taking above considerations into accounts, the soft carbon-hierarchical porous carbon cell can be the most promising candidate for the advanced SICs. As it is widely known, soft carbon usually provides a sufficient capacity ($< 1.0 \text{ V vs Na/Na}^+$) and good rate capability. As for the hierarchical porous carbon cathode, it exhibits triangular charge-discharge profiles in the potential range of $1.5\text{--}4.2 \text{ V}$ versus Na/Na^+ , which can offer a high capacity. In a word, the soft carbon-hierarchical porous carbon cell may be the most promising candidate for the next-generation carbon-based hybrid capacitors and is worthy of deeper investigations.

Acknowledgements

This work was financially supported by the National Key Research and Development Program of China (2018YFC1901605), National Natural Science Foundation of China (52004338), Hunan Provincial Natural Science Foundation of China (2020JJ5696), and Guangdong Provincial Department of Natural Resources (2020-011).

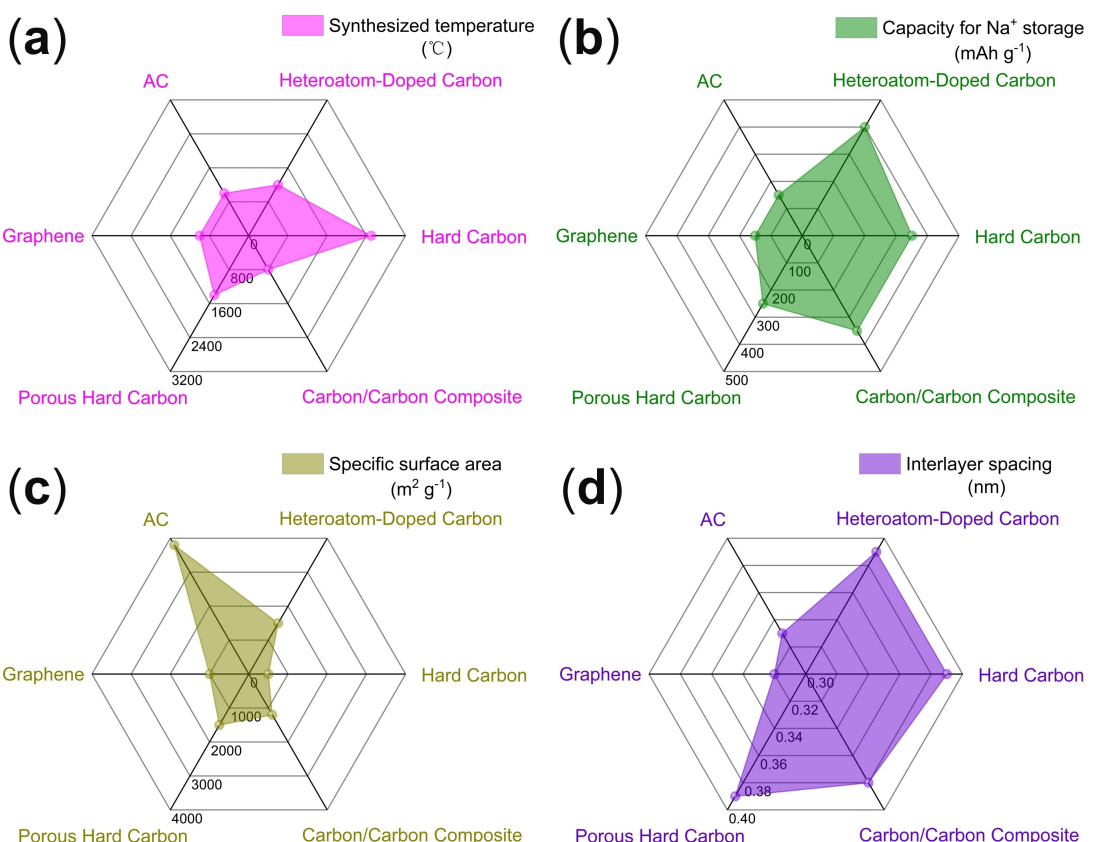


Figure 12. Key parameters of Cathode carbon materials (AC, graphene, and porous hard carbon) and anode carbon materials (hard carbon, heteroatom-doped carbon, and carbon/carbon composite) for SICs. a) The synthesized temperature, b) capacity of Na^+ storage, c) SSA, and d) the interlayer spacing.

Conflict of Interest

The authors declare no conflict of interest.

Keywords: sodium-ion capacitors • carbon materials • hybrid capacitors • sodium-ion storage • electrochemistry

- [1] J. Ge, B. Wang, J. Wang, Q. Zhang, B. Lu, *Adv. Energy Mater.* **2019**, *10*, 1903277.
- [2] Z. Xia, H. Sun, X. He, Z. T. Sun, C. Lu, J. Li, Y. Peng, S. X. Dou, J. Y. Sun, Z. F. Liu, *Nano Energy* **2019**, *60*, 385.
- [3] L. Xu, J. Li, W. Deng, H. Shuai, S. Li, Z. Xu, J. Li, H. Hou, H. Peng, G. Zou, X. Ji, *Adv. Energy Mater.* **2020**, DOI: 10.1002/aenm.202000648.
- [4] A. Manthiram, *Nat. Commun.* **2020**, *11*, 1550.
- [5] J. Xiao, Q. Li, Y. Bi, M. Cai, B. Dunn, T. Glossmann, J. Liu, T. Osaka, R. Sugiura, B. Wu, J. Yang, J.-G. Zhang, M. S. Whittingham, *Nat. Energy* **2020**, *5*, 561.
- [6] K. Chayambuka, G. Mulder, D. L. Danilov, P. H. L. Notten, *Adv. Energy Mater.* **2020**, DOI: 10.1002/aenm.202001310.
- [7] X. Wang, L. Liu, Z. Niu, *Mater. Chem. Front.* **2019**, *3*, 1265.
- [8] G. Li, Z. Yang, Z. Yin, H. Guo, Z. Wang, G. Yan, Y. Liu, L. Li, J. Wang, *J. Mater. Chem. A* **2019**, *7*, 15541.
- [9] Y. Zhang, J. Jiang, Y. An, L. Wu, H. Dou, J. Zhang, Y. Zhang, S. Wu, M. Dong, X. Zhang, Z. Guo, *ChemSusChem* **2020**, *13*, 2522.
- [10] Z. Li, L. Cao, W. Chen, Z. Huang, H. Liu, *Small* **2019**, *15*, 1805173.
- [11] G. G. Amatucci, F. Badway, A. Du Pasquier, T. Zheng, *J. Electrochem. Soc.* **2001**, *148*, A930.
- [12] S. Natarajan, Y. S. Lee, V. Aravindan, *Chem. Asian J.* **2019**, *14*, 936.
- [13] X. Wu, Y. Chen, Z. Xing, C. W. K. Lam, S. S. Pang, W. Zhang, Z. Ju, *Adv. Energy Mater.* **2019**, *9*, 1900343.
- [14] W. Zhang, Y. Liu, Z. Guo, *Sci. Adv.* **2019**, *5*, 7412.
- [15] H. Zhang, M. Hu, Q. Lv, Z. H. Huang, F. Kang, R. Lv, *Small* **2020**, *16*, 1902843.
- [16] J. Ding, H. Wang, Z. Li, K. Cui, D. Karpuзов, X. Tan, A. Kohandehghan, D. Mitlin, *Energy Environ. Sci.* **2015**, *8*, 941.
- [17] B. Yang, J. Chen, S. Lei, R. Guo, H. Li, S. Shi, X. Yan, *Adv. Energy Mater.* **2018**, *8*, 1702409.
- [18] Y. Shao, M. F. El-Kady, J. Sun, Y. Li, Q. Zhang, M. Zhu, H. Wang, B. Dunn, R. B. Kaner, *Chem. Rev.* **2018**, *118*, 9233.
- [19] B. Wang, Z. Deng, Y. Xia, J. Hu, H. Li, H. Wu, Q. Zhang, Y. Zhang, H. Liu, S. Dou, *Adv. Energy Mater.* **2019**, *10*, 1903119.
- [20] P. Simon, Y. Gogotsi, *Nat. Mater.* **2020**, *19*, 1151.
- [21] S. Chen, Q. Kuang, H. J. Fan, *Small* **2020**, *16*, 2002803.
- [22] R. Fei, H. Wang, Q. Wang, R. Qiu, S. Tang, R. Wang, B. He, Y. Gong, H. J. Fan, *Adv. Energy Mater.* **2020**, DOI: 10.1002/aenm.202002741.
- [23] J. Yin, L. Qi, H. Wang, *ACS Appl. Mater. Interfaces* **2012**, *4*, 2762.
- [24] Z. Chen, V. Augustyn, X. Jia, Q. Xiao, B. Dunn, Y. Lu, *ACS Nano* **2012**, *6*, 4319.
- [25] K. Kuratani, M. Yao, H. Senoh, N. Takeichi, T. Sakai, T. Kiyobayashi, *Electrochim. Acta* **2012**, *76*, 320.
- [26] J. Tang, X. Huang, T. Lin, T. Qiu, H. Huang, X. Zhu, Q. Gu, B. Luo, L. Wang, *Energy Storage Mater.* **2020**, *26*, 550.
- [27] A. M. Glushenkova, A. V. Ellis, *Adv. Sustainable Syst.* **2018**, *2*, 1800006.
- [28] D. Xu, D. Chao, H. Wang, Y. Gong, R. Wang, B. He, X. Hu, H. J. Fan, *Adv. Energy Mater.* **2018**, *8*, 1702769.
- [29] Y. Shao, J. Xiao, W. Wang, M. Engelhard, X. Chen, Z. Nie, M. Gu, L. V. Saraf, G. Exarhos, J. G. Zhang, J. Liu, *Nano Lett.* **2013**, *13*, 3909.
- [30] H. Hou, X. Qiu, W. Wei, Y. Zhang, X. Ji, *Adv. Energy Mater.* **2017**, *7*, 1602898.
- [31] Y. Gogotsi, R. M. Penner, *ACS Nano* **2018**, *12*, 2081.
- [32] K. Zou, P. Cai, X. Cao, G. Zou, H. Hou, X. Ji, *Curr. Opin. Electrochem.* **2020**, *21*, 31.
- [33] D. Saurel, B. Orayech, B. Xiao, D. Carriazo, X. Li, T. Rojo, *Adv. Energy Mater.* **2018**, *8*, 1703268.
- [34] J. Ajuria, E. Redondo, M. Arnaiz, R. Mysyk, T. Rojo, E. Goikolea, *J. Power Sources* **2017**, *359*, 17.
- [35] P. Cai, K. Zou, G. Zou, H. Hou, X. Ji, *Nanoscale* **2020**, *12*, 3677.
- [36] J. Xu, Z. Liu, F. Zhang, J. Tao, L. Shen, X. Zhang, *RSC Adv.* **2020**, *10*, 7780.
- [37] H. Li, J. Lang, S. Lei, J. Chen, K. Wang, L. Liu, T. Zhang, W. Liu, X. Yan, *Adv. Funct. Mater.* **2018**, *28*, 1800757.
- [38] B. Wang, T. Ruan, Y. Chen, F. Jin, L. Peng, Y. Zhou, D. Wang, S. Dou, *Energy Storage Mater.* **2020**, *24*, 22.
- [39] H. Huang, H. Shi, P. Das, J. Qin, Y. Li, X. Wang, F. Su, P. Wen, S. Li, P. Lu, F. Liu, Y. Li, Y. Zhang, Y. Wang, Z. S. Wu, H. M. Cheng, *Adv. Funct. Mater.* **2020**, *30*, 1909035.
- [40] J. Zhang, W. Lv, Y. Tao, Y.-B. He, D.-W. Wang, C.-H. You, B. Li, F. Kang, Q.-H. Yang, *Energy Storage Mater.* **2015**, *1*, 112.
- [41] Y. Liu, B. V. Merinov, W. A. Goddard, *3rd Proc. Natl. Acad. Sci. USA* **2016**, *113*, 3735.
- [42] J. Zhang, W. Lv, D. Zheng, Q. Liang, D.-W. Wang, F. Kang, Q.-H. Yang, *Adv. Energy Mater.* **2018**, *8*, 1702395.
- [43] K. Zou, P. Cai, B. Wang, C. Liu, J. Li, T. Qiu, G. Zou, H. Hou, X. Ji, *Nano-Micro Lett.* **2020**, DOI: 10.1007/s40820-020-00458-6.
- [44] S. Dong, Y. Xu, L. Wu, H. Dou, X. Zhang, *Energy Storage Mater.* **2018**, *11*, 8.
- [45] H. Ma, H. Geng, B. Yao, M. Wu, C. Li, M. Zhang, F. Chi, L. Qu, *ACS Nano* **2019**, *13*, 9161.
- [46] S. Chen, J. Wang, L. Fan, R. Ma, E. Zhang, Q. Liu, B. Lu, *Adv. Energy Mater.* **2018**, *8*, 1800140.
- [47] X. Wang, S. He, F. Chen, X. Hou, *Energy Fuels* **2020**, *34*, 13144.
- [48] F. Li, Z. Zhou, *Small* **2018**, *14*, 1702961.
- [49] S. Qiu, L. Xiao, M. L. Sushko, K. S. Han, Y. Shao, M. Yan, X. Liang, L. Mai, J. Feng, Y. Cao, X. Ai, H. Yang, J. Liu, *Adv. Energy Mater.* **2017**, *7*, 1700403.
- [50] K. Kubota, S. Shimadzu, N. Yabuuchi, S. Tominaka, S. Shiraishi, M. Abreu-Sepulveda, A. Manivannan, K. Gotoh, M. Fukunishi, M. Dahbi, S. Komaba, *Chem. Mater.* **2020**, *32*, 2961.
- [51] F. Wang, X. Wang, Z. Chang, X. Wu, X. Liu, L. Fu, Y. Zhu, Y. Wu, W. Huang, *Adv. Mater.* **2015**, *27*, 6962.
- [52] H. Liu, X. Liu, H. Wang, Y. Zheng, H. Zhang, J. Shi, W. Liu, M. Huang, J. Kan, X. Zhao, D. Li, *ACS Sustainable Chem. Eng.* **2019**, DOI: 10.1021/acssuschemeng.9b01370.
- [53] Z. Xu, M. Wu, Z. Chen, C. Chen, J. Yang, T. Feng, E. Paek, D. Mitlin, *Adv. Sci.* **2019**, *6*, 1802272.
- [54] K. Liao, H. Wang, L. Wang, D. Xu, M. Wu, R. Wang, B. He, Y. Gong, X. Hu, *Nanoscale Adv.* **2019**, *1*, 746.
- [55] G. H. Dong, H. L. Wang, W. Liu, J. Shi, S. J. Sun, D. Li, H. Zhang, Y. P. Yang, Y. P. Cui, *ACS Appl. Energy Mater.* **2018**, *1*, 5636.
- [56] C. Yang, M. Zhang, N. Kong, J. Lan, Y. Yu, X. Yang, *ACS Sustainable Chem. Eng.* **2019**, *7*, 9291.
- [57] R. Thangavel, A. G. Kannan, R. Ponraj, G. Yoon, V. Aravindan, D.-W. Kim, K. Kang, W.-S. Yoon, Y.-S. Lee, *Energy Storage Mater.* **2020**, *25*, 702.
- [58] R. Yan, E. Josef, H. Huang, K. Leus, M. Niederberger, J. P. Hofmann, R. Walczak, M. Antonietti, M. Oschatz, *Adv. Funct. Mater.* **2019**, *29*, 1902858.
- [59] C.-C. Chen, J. Maier, *Nat. Energy* **2018**, *3*, 102.
- [60] R. Yan, K. Leus, J. P. Hofmann, M. Antonietti, M. Oschatz, *Nano Energy* **2020**, *67*, 104240.

Manuscript received: November 27, 2020

Revised manuscript received: December 11, 2020

Accepted manuscript online: December 13, 2020

Version of record online: January 18, 2021